



## LABORATORY STUDY ON LOESS LIQUEFACTION

LANMIN WANG ZHENZHONG ZHANG LAN LI and JUN WANG

Seismological Institute of Lanzhou, State Seismological Bureau (SSB),  
Panxuan Road, Lanzhou 730000, P. R. China

### ABSTRACT

The latest field investigation of earthquake disasters and laboratory tests have revealed that loess has enormous potentialities of liquefaction and flow failure. In this paper, the mechanism, failure standard and key factors of influencing loess liquefaction were studied, based on the dynamic triaxial tests of saturated undisturbed loess samples secured from the Northwestern China under irregular seismic loadings and sinusoidal loading respectively. The mathematic models for the developments of both pore water pressure and axial residual strain under cyclic sinusoidal loading were established.

### KEYWORDS

Loess liquefaction; seismic loading; dynamic triaxial test.

### INTRODUCTION

Loess is a sort of weak cohesive soil with porous microstructure formed in Quaternary. It is widely distributed in the northwestern China, with the thickness of 50-300 m, where many strong earthquakes occurred and all the historical strong earthquakes induced serious geotechnical disasters. Among them, seismic landslides and seismic subsidence have already been studied in detail by some investigators. But liquefaction of loess has not been paid more attention and the information in regard to it is limited. However, the recent field investigation of earthquake disasters and laboratory tests (Ishihara *et al.*, 1990; Lanmin W. *et al.*, 1994) have revealed that loess has enormous potentialities of liquefaction and flow failure. This type of failure is generally progressive to develop in soil, which only requires small magnitude of driving force to induce disasters.

## APPARATUS, SPECIMENS AND LOADINGS USED IN THE TEST

By use of a magnetic dynamic triaxial test apparatus, which can apply an axial loading with arbitrary waveforms in a frequency range of 0-100 Hz on a specimen, liquefaction tests were performed for 195 undisturbed specimens with the diameter of 5 cm and the length of 10 cm, secured from the depth of 5-20 meters of loess deposit formed in the late period of Pleistocene ( $Q_3$ ), which is called Malan loess. The physical parameters of the specimens are presented in Table 1. Irregular seismic loadings and cyclic sinusoidal loading with the frequency of 1 Hz were directly applied on a specimen in the tests. The parameters of the irregular seismic loadings are presented in Table 2.

Table 1. The physical parameters of the specimens used in the tests

Sample number	Physical parameters				Gradation (%)		
	Water content (%)	Unit weight (kN/m <sup>3</sup> )	Void ratio	Plasticity index	Clay	Silt	Sand
L94-1	7.92-9.00	13.7-14.9	0.865-1.069	8.4-10	10	78	12
L94-2	9.1	14.4	1.061	9.8	13	64.7	22.3
L95-3	14-20	14.6-15.8	1.17-1.3	6-10	16	53	33
L95-4	12-18	14.3-16.2	0.8-1.15	9	13.5	70.5	16.0

Table 2. The parameters of irregular seismic loadings

Loading number	Predominant period (s)	Duration (s)	Loading type	Seismic intensity (in 12 degrees)	Probability of exceedance	Site
1	0.2	7	shock	7		loess
2	0.1	6.4	cyclic	6		hard soil
3	0.17	15	cyclic	8	10% in 50 yrs.	bedrock
4	0.15	20	cyclic	8.5	10% in 100 yrs.	bedrock
5	0.20	19	cyclic	8	10% in 50 yrs.	bedrock
6	0.50	25.5	cyclic	8.5	10% in 50 yrs.	loess

In Table 1, No. 1 and No. 2 loadings are respectively NS-component of horizontal accelerations registered at Cymbulif during the main shock of the Tajik 5.5 earthquake in 1989 and UD-component of the 5.3 aftershock during the Longling earthquake of China in 1974. The loadings of No. 3 to No. 6 are artificial seismic waves or seismic response wave at 3 sites of Gansu province, China.

## THE MECHANISM AND STANDARD OF LOESS LIQUEFACTION

The test result shown that loess liquefaction is not completely the same as sand liquefaction. There are two obvious differences between them. First, during liquefaction of saturated loess, the pore

water pressure can not develop to the confining stress under homogenous consolidation, which generally increases to about 70% of the effective confining stress shown as Fig. 1. Second, when saturated loess liquefies, greater residual strain in the range of 3%-20% develops shown as Fig. 2.

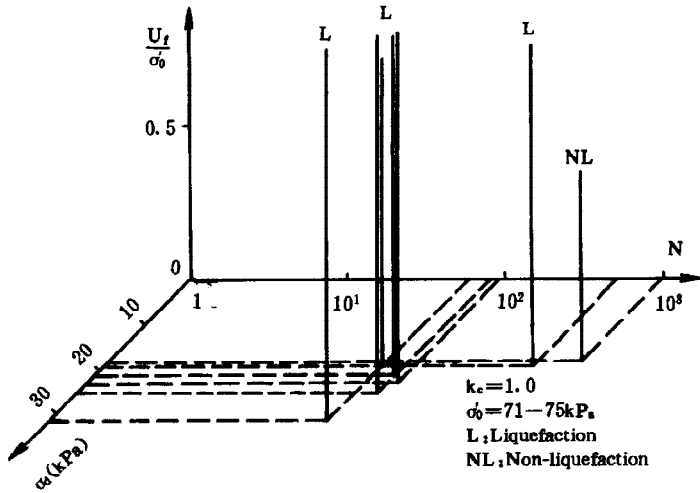


Fig. 1. The maximum pore water pressures during liquefaction of loess specimens

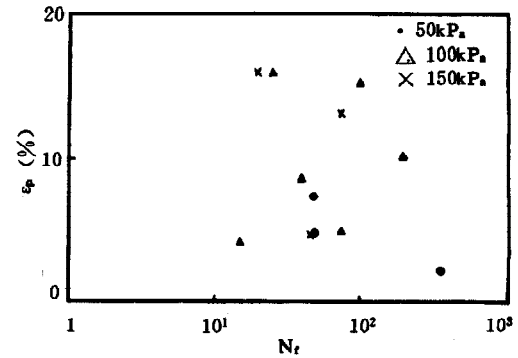


Fig. 2. Residual strain during liquefaction of loess specimens.

The behaviour mainly depends on the weak cohesive and porous microstructure of loess. Under the saturated state, the middle and small-sized pores of loess are filled with water. A part of big-sized pores do the same. But most of mini-sized pores are not filled with water. Under the effect of dynamic loading, the development of pore water pressure expresses as three stages in Fig. 3. In the first stage, the microstructure of loess is basically in a good state and the strain mainly develops in

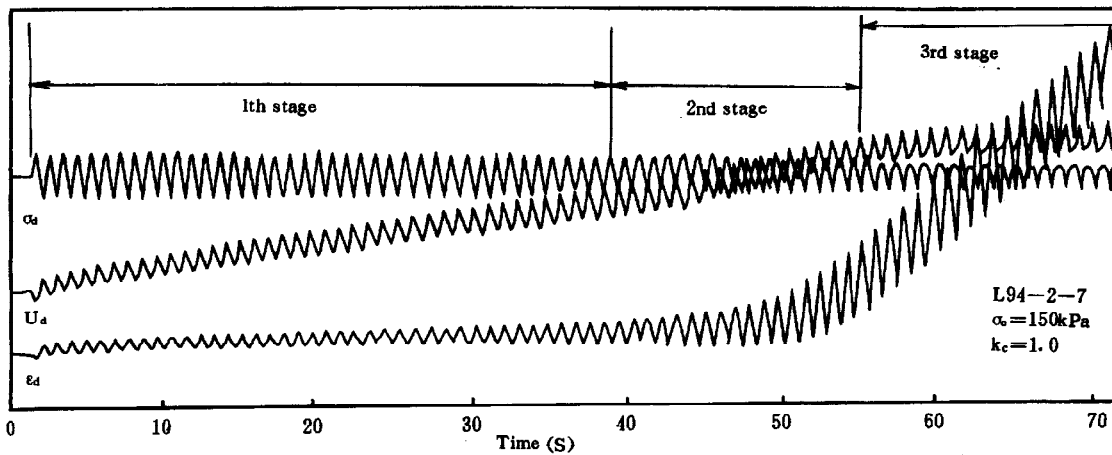


Fig. 3. The typical time histories of stress, strain and pore water pressure recorded in the test.

an elastic range, the corresponding pore water pressure is called elastic one. With the damage of porous microstructure of loess, slit particles separate to fall into the pores. The volume of pores dramatically decrease. The water in the pores can not drain out in the moment so as to cause the pore water pressure to increase, which induces the effective stress applying on the framework of soil and the strength of loess to lose greatly. This is the second stage, in which pore water pressure is called

structural one or residual one. On the other hand, the pore water can enter a part of big and mini-sized pores in the process of pore water pressure increasing, which dissipates the water pressure in the middle and small-sized pores filled originally with water in a certain extent. This is the third stage, in which the pore water pressure is called transmitting one. The transmitting of pore water pressure limits the increasing of it so that the pore water pressure can not reach the effective confining stress. However, higher residual pore pressure and greater residual strain still develops in loess specimens due to the damage of porous microstructure and redistribution of the effective stress.

Considering the above-mentioned two differences and failure strain of microstructure of 3% for loess, it may be acceptable to adopt a criterion of pore water pressure building up to 70% of initial effective confining pressure to define initial liquefaction of loess and a criterion of 3% axial strain or pore water pressure developing to 70% of initial effective confining pressure (whichever stage comes earlier) to define failure of loess induced by liquefaction. This test result is slightly different with that of the loessial soil in the middle part of America (Shamsher P. *et. al.*, 1982).

## CONDITIONS CAUSING LIQUEFACTION OF LOESS

### *Site Conditions*

The field investigations respectively for the liquefaction-induced sliding flow of loess deposit in Shibeiyuan, Ningxia province of China caused by the Haiyuan 8.5 earthquake in 1920 by the authors and for the liquefaction—induced a large scale of mud flow caused by the Tajik 5.5 earthquake in 1989 by Ishihara K. shown that liquefaction of loess requires two essential site conditions. One is having the integrated loess deposit formed in the late period of Pleistocene (Q3), which is called Malan loess, with the topography of smooth landform or gentle slope. The other is supplying of underground water or the other water sources such as agricultural irrigation water.

The liquefaction of loess in Shibeiyuan occurred in the integrated Malan loess deposit on the second and third terraces with the levels of underground water of respectively 5-10 m and 10-20 m. During the earthquake, rising of underground water made sandy loess layer and sand layer in the depth of 10-16 m saturated. Under the effect of the earthquake, the soil body of gentleslope with the slope of 2.5% slid forward for 1.5 km. The liquefaction of loess in Tajik also happened in the wind laid loess deposit (Malan loess) on the nearly smooth site in a gentle slope and hilly area. Before the earthquake, due to agricultural irrigation, the loess deposit in the depth of 5-20 m saturated or over-saturated. Under the effect of the earthquake, liquefaction induced a large scale of mud flow.

### *Water Content Condition*

The test research shown that water content is the most important factor of influencing liquefaction of

loess. It is found that, if water content of loess is higher than its plastic limit, the pore water pressure may obviously increase under the seismic stress to express as partly liquefaction or completely liquefaction shown as Fig. 4. That is to say, when water content of loess deposit is higher than its plastic limit, the loess deposit has a liquefaction potential.

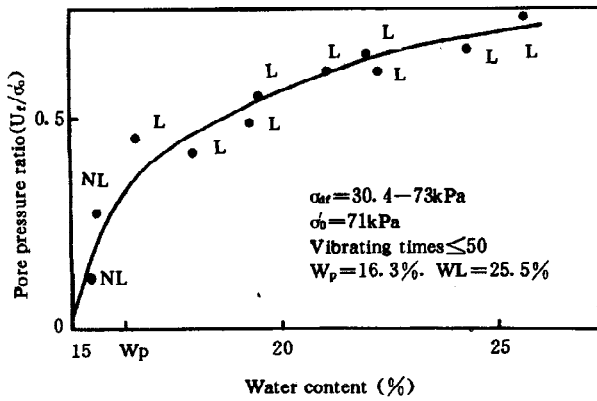


Fig. 4. Influence of water content on liquefaction of loess.

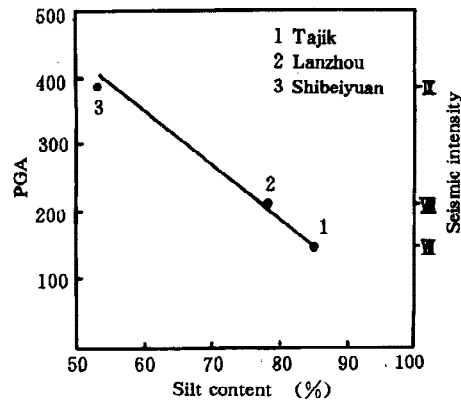


Fig. 5. Influence of silt content on PGA triggering liquefaction of loess.

#### Ground Motion Intensity Condition

Besides the site and water content conditions, liquefaction of loess must require an extra triggering condition, i. e., condition of ground motion intensity. The back-analysis and prediction for liquefaction cases shown that PGA required by triggering liquefaction has a close relationship with silt content (SP) of loess shown as Fig. 5. The relationship can be described by the following formula:

$$PGA = -8.0623 \cdot SP + 835.3 \quad (1)$$

#### THE MODELS FOR DEVELOPMENT OF PORE WATER PRESSURE AND RESIDUAL STRAIN

##### The Models for Development of Pore Water Pressure

The test result presented in Fig. 6(a), (b), (c) shows that under homogenous consolidation stress, the confining stress ( $\sigma_0$ ) has a predominant effect on the curve of pore water pressure ratio ( $U_d/U_t$ ) versus vibration times ratio ( $N/N_f$ ). If  $\sigma_0$  is less than the original overburden pressure ( $\sigma_v$ ), the curve of  $U_d/U_t - N/N_f$  may be described with power function in equation (2).

$$\frac{U_d}{U_t} = \left(\frac{N}{N_f}\right)^b \quad \sigma_0 < \sigma_v \quad (2)$$

where  $b$  is a constant from the test, generally,  $0 < b < 1$ .

If  $\sigma_0 = \sigma_v$  or  $\sigma_0 > \sigma_v$ , the shapes of the curves are different for different vibration times. They can be described respectively with the following equation (3) and (4).

$$\frac{U_d}{U_r} = \begin{cases} \left( \frac{N}{N_r} \right)^b; & N \leq 20 \\ \left[ \cos \left( \frac{\pi}{2} \left( \frac{N}{N_r} - 1 \right) \right) \right]^b; & 20 < N_r \leq 50 \\ \left. \begin{aligned} & \frac{1}{2} + \frac{1}{\pi} \sin^{-1} \left[ 2 \left( \frac{N}{N_r} \right)^{\alpha_1} - 1 \right]; & 0 \leq \frac{N}{N_r} \leq 0.5 \\ & 2 \frac{N}{N_r} - \left\{ \frac{1}{2} + \frac{1}{\pi} \sin^{-1} \left[ 2 \left( \frac{N}{N_r} \right)^{\alpha_2} - 1 \right] \right\}; & 0.5 < \frac{N}{N_r} \leq 1.0 \end{aligned} \right\} & 50 < N_r \leq 200, \sigma_0 = \sigma_v \\ \frac{1}{2} + \frac{1}{\pi} \sin^{-1} \left[ 2 \left( \frac{N}{N_r} \right)^{\alpha} - 1 \right]; & N_r > 200 \end{cases} \quad (3)$$

where,  $a$ ,  $b$ ,  $\alpha_1$ ,  $\alpha_2$  and  $\alpha$  are constants from the test.

$$\frac{U_d}{U_r} = \begin{cases} \left( \frac{N}{N_r} \right)^b; & N_r \leq 20 \\ \left[ \cos \frac{\pi}{2} \left( \frac{N}{N_r} - 1 \right) \right]^b; & 20 < N_r \leq 50 \\ 50 < N_r < 200, \text{ the same as (3)} \\ N_r \geq 200, \text{ the same as (3)} \end{cases} \quad \sigma_0 > \sigma_v \quad (4)$$

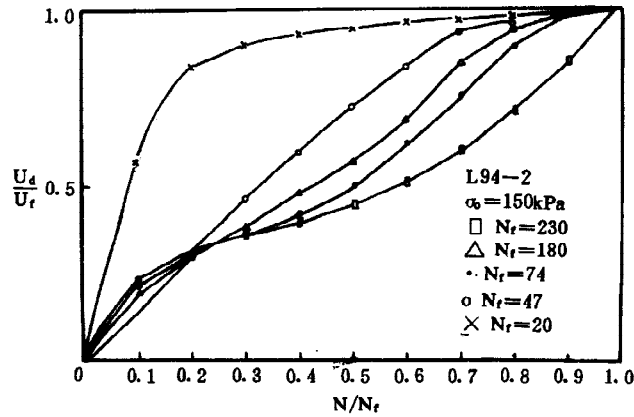
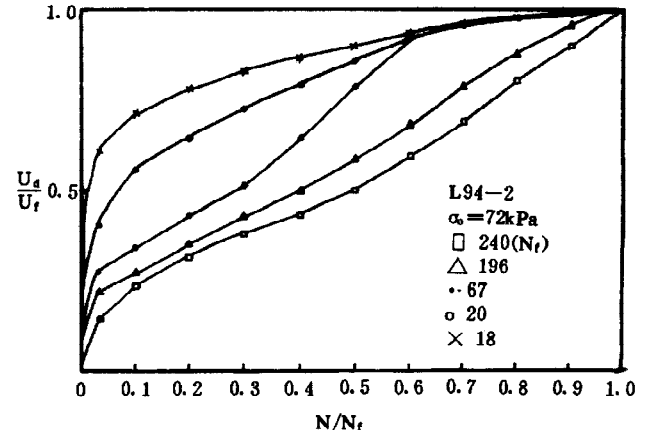
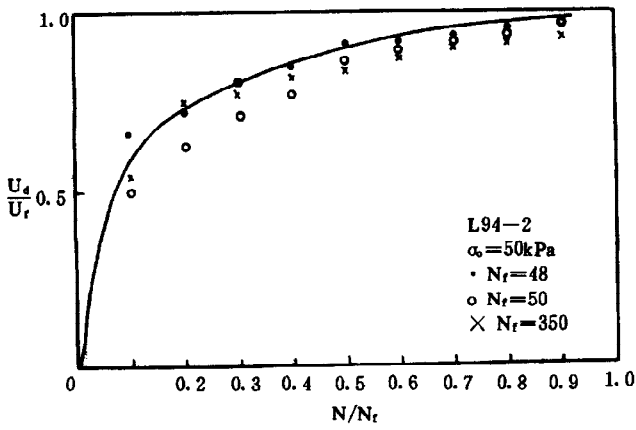


Fig. 6. The curves of  $U_d/U_r$  versus  $N/N_r$ .

## The Model for Development of Residual Strain

Seismic subsidence may develop in intact unsaturated loess deposit, which is generally expressed with residual strain in soil dynamics. This type of sudden settlement is much more predominant for saturated loess specimens. Fig. 7 shows that the curves of residual strain ratio ( $\epsilon_p/\epsilon_t$ ) versus vibration times ratio ( $N/N_t$ ) under different confining stress and vibration times of liquefaction have similar shape, which may be described by the following exponent function:

$$\frac{\epsilon_p}{\epsilon_t} = a \left( \frac{N}{N_t} - 1 \right) \quad (5)$$

where  $a$  is a constant from the test, generally,  $a > 1$ .

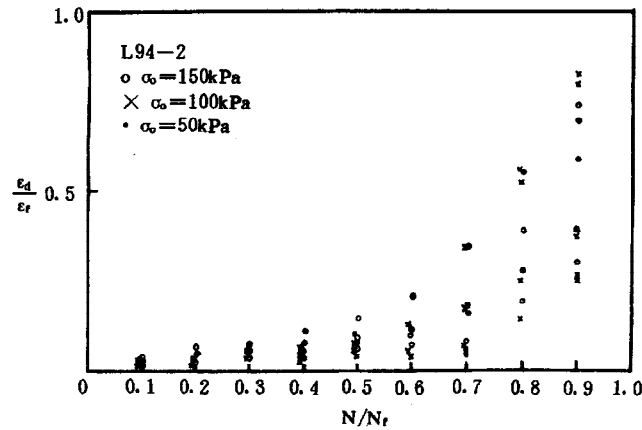


Fig. 7. The curves of  $\epsilon_p/\epsilon_t$  versus  $N/N_t$ .

## Examination of The Models

In order to examine the formulae of (2) to (5), the tested curves and calculated curves of pore water pressure and residual strain were respectively compared in Fig. 8 and Fig. 9. In the two figures, the

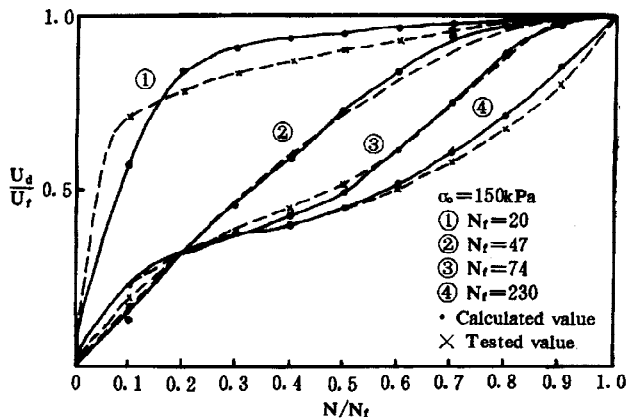


Fig. 8. Examination of the models for pore water pressure development

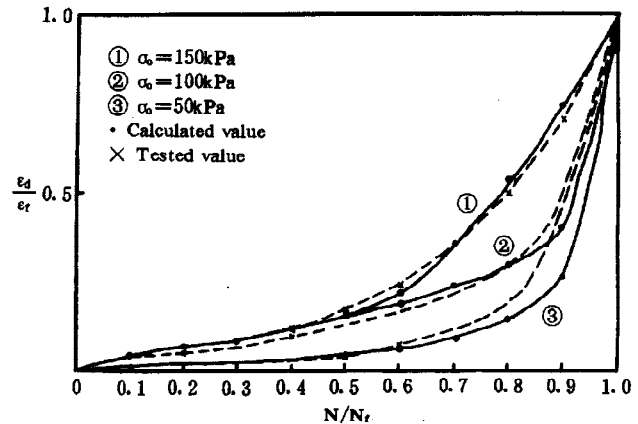


Fig. 9. Examination of the models for residual strain development.

dash lines come from calculation with the models, and the solid lines come from test. The relevant differences are basically less than 10%. Obviously, these models prove to be suitable for loess.

The irregular seismic loadings presented in Table. 2 were directly used to perform the dynamic triaxial test of liquefaction. The test result shown that the key parameters of seismic loadings have obvious influence on the development of pore water pressure. Under the effect of the seismic loading with shock type, there is "jump" phenomena in the process of pore water pressure development. This "jump" only cause increasing or decreasing of elastic pore water pressure and do not changes the shape of the curves of  $U_d/U_t - N/N_t$ . However, there is no the "jump" under the seismic loading with cyclic type. No matter what type of seismic loading, the greater the amplitude of seismic loading is, the faster the development of pore water pressure is. The dynamic stress needed by triggering liquefaction decreases with the predominant period and duration of seismic loading becoming long.

### CONCLUSION

- (1). The mechanism of loess liquefaction is not completely the same as that of sand liquefaction, which depends on the porous microstructure with weak cohesion of loess. Therefore, it is necessary to study further the detailed mechanism of it.
- (2). The site condition and water content condition are internal causes of loess liquefaction. The ground motion intensity condition is external cause of it. These three conditions can be taken as criterions of liquefaction of loess site.
- (3). The curves of pore water pressure ratio versus vibration times ratio under different consolidation stress may be respectively described with power founction, exponent founction, triangular founction and inverse triangular founction or their combinations.
- (4). The type (shock or cyclic), amplitude, predominant period and duration of an irregular seismic loading has an obvious effect on the development of pore water pressure and the critical dynamic stress needed by triggering liquefaction.

### ACKNOWLEDGEMENT

The authors wish to thank for the financial support of Seismology Joint Foundation of China.

### REFERENCE

- Ishihara K . , Okusa S . , Oyagi N . and Ischuk A . ( 1 9 9 0 ) . Liquefaction - induced flow slide in the collapsible loess deposit in Soviet Tajik , *Soil and Foundations*. 30, No. 4, pp. 73-89.
- Lanmin W . , Jun W . and Lan L . ( 1 9 9 4 ) . Laboratory prediction of loess liquefaction under irregular seismic loadings. *Proc. The Fouth National Conference on Soil Dynamics*. pp. 134-137.
- Shamsher P . and Vijay K . P . ( 1 9 8 2 ) . Liquefaction of loessial soils , *Proc . 3 th International Earthquake Microzonation Conference*. 2, pp. 1101-1107.